УДК 551.465

© *В. А. Зинченко*[1,2], *С. М. Гордеева*[1,2,3], *Ю. В. Собко*[4], *Т. В. Белоненко*[1]

© Перевод *Е. С. Кочеткова,* 2019

[1] Санкт-Петербургский государственный университет, г. Санкт-Петербург

[2] Российский государственный гидрометеорологический университет, г. Санкт-Петербург

[3] Институт океанологии им. П.П. Ширшова РАН, г. Москва

[4] Deutsche Telekom, стратегическое подразделение в Санкт-Петербурге, г. Санкт-Петербург

btvlisab@yandex.ru

МЕЗОМАСШТАБНЫЕ ВИХРИ ЛОФОТЕНСКОЙ КОТЛОВИНЫ ПО СПУТНИКОВЫМ ДАННЫМ

Статья поступила в редакцию 11.03.2019, после доработки 02.07.2019

Изучаются мезомасштабные вихри Лофотенской котловины Норвежского моря. Алгоритм автоматической идентификации и трекинга вихрей применяется к спутниковым альтиметрическим данным. За период 1993–2017 гг. в Лофотенской котловине выявлено 166 000 циклонических и 169 395 антициклонических случаев проявления мезомасштабных вихрей, к которым в дальнейшем была применена процедура связывания в треки. Дальнейший анализ производился по трекам долгоживущих (время жизни более 35 сут) вихрей: 120 циклонических и 210 антициклонических вихрей. Анализировалось пространственное распределение мезомасштабных вихрей в Лофотенской котловине, выделены очаги их генерации и диссипации, проведен статистический анализ их характеристик. Показано, что в Лофотенской котловине существуют различные районы проявления мезомасштабных вихрей, которые могут отражать разный механизм их образования: отрыв от Норвежского течения при его меандрировании и генерация вихрей непосредственно в Лофотенской котловине. Во фронтальной зоне Норвежского течения существуют три выраженные области формирования вихрей, откуда они смещаются на запад и северо-запад, формируя три основных траектории. Показано, что вблизи Лофотенского вихря доминируют антициклонические вихревые образования. Однако циклонические вихревые структуры вблизи Лофотенского вихря также встречаются в достаточном количестве и локализуются в окрестности двух точек с центрами 69.5° с.ш., 4° в.д. и 70° с.ш., 2.5° в.д. Эти циклонические вихри, как правило, являются долгоживущими и находятся в области с циклонической завихренностью, окружая Лофотенский вихрь (shielded vortex). Мезомасштабные вихри, приходящие в зону Лофотенского вихря извне, образуются преимущественно в области Норвежского течения и перемещаются, как правило, в циклоническом направлении. Применив алгоритм автоматической идентификации и трекинга вихрей, мы показали, что антициклонические мезомасштабные вихри в Лофотенской котловине образуются в большинстве своем во фронтальной зоне Норвежского течения, диссипируя не очень далеко от места своего образования, в то время как циклонические вихри могут образоваться в разных местах акватории Лофотенской котловины. В западной части котловины вихрей значительно меньше, чем в других ее частях.

Ключевые слова: Норвежское море, Лофотенский вихрь, Лофотенская котловина, мезомасштабные вихри, альтиметрия, автоматическая идентификация, трекинг, экранированные вихри.

V. A. Zinchenko[1,2], *S. M. Gordeeva*[1,2,3], *Yu.V. Sobko*[4], *T. V. Belonenko*[1]

[1] St.-Petersburg State University, St.-Petersburg, Russia

[2] Russian State Hydrometeorological University, St.-Petersburg, Russia

[3] Shirshov Institute of Oceanology of the Russian Academy of Sciences, Moscow, Russia

[4] Deutsche Telekom, St.-Petersburg, Russia

ANALYSIS OF MESOSCALE EDDIES IN THE LOFOTEN BASIN BASED ON SATELLITE ALTIMETRY

Received 11.03.2019, in final form 02.07.2019

We studied mesoscale eddies in the Lofoten Basin of the Norwegian Sea. The automatic eddy identification and tracking algorithm were applied to satellite altimetry. Images of 166,000 cyclonic and 169,395 anticyclonic eddies were detected in the Lofoten Basin from 1993 to 2017, then the tracking procedure was applied to them. We analyzed tracks of long-lived (lifetime more than 35 days) individual eddies. They are 120 cyclonic and 210 anticyclonic eddies. We studied

Ссылка для цитирования: *Зинченко В.А.*, *Гордеева С.М.*, *Собко Ю.В.*, *Белоненко Т.В.* Мезомасштабные вихри Лофотенской котловины по спутниковым данным // Фундаментальная и прикладная гидрофизика. 2019. Т. 12, № 3. С. 46–54

For citation: *Zinchenko V.A.*, *Gordeeva S.M.*, *Sobko Yu.V.*, *Belonenko T.V.* Analysis of Mesoscale eddies in the Lofoten Basin based on satellite altimetry. *Fundamentalnaya i Prikladnaya Gidrofizika*. 2019, 12, 3, 46–54

DOI: 10.7868/S2073667319030067

a spatial distribution of mesoscale eddies in the Lofoten Basin as well as locations of their generation and dissipation. A statistical analysis of their characteristics also was carried out. We show that two predominant systems of mesoscale eddy formation exist in the Lofoten Basin. This fact may reflect two different mechanisms of eddy generation. The first one is the separation of eddies from the Norwegian current during its meandering. The second one is the direct generation of eddies inside the Lofoten Basin. There are three distinct areas of eddy generation in the frontal zone of the Norwegian current, from where eddies move to the west and north-west, forming three main trajectories. Anticyclonic eddies dominate in the area of the Lofoten vortex. Having arisen, they rotate intensively within the area of the Lofoten vortex in the anticyclonic gyre and interact obviously with the Lofoten vortex by merging. However, cyclonic eddies structures in the area of the Lofoten vortex are also found in a sufficient amount, and they are localized in the vicinity of two points with centers of 69.5° N, 4° E, and 70° N, 2.5° E. These cyclonic eddies are located in an area with cyclonic vorticity surrounding the Lofoten vortex like an annulus (shielded vortex). Mesoscale eddies that enter the area of the Lofoten vortex from outside are formed mainly in the region of the Norwegian current and tend to have the cyclonic rotation. We demonstrate that anticyclonic mesoscale eddies in the Lofoten Basin are formed mostly in the frontal zone of the Norwegian current and decay not too far from the place of their formation, while cyclonic eddies can form in different places in the Lofoten Basin. The number of eddies is much smaller in the western part of the Lofoten Basin than in other parts of it.

Keywords: Norwegian Sea, Lofoten vortex, Lofoten Basin, mesoscale eddies, altimetry, automatic identification, tracking, shielded vortex.

The Lofoten Basin (LB) is a lowering in the Norwegian Sea bottom relief with a maximum depth of 3250 m. Its water area is limited to coordinates of 5° W–20° E and 64–76° N – between the Mohn ridge in the northwest and the Scandinavian Peninsula in the east, in the south, it is adjacent to the Vøring Plateau (fig. 1, see Insert). The LB is the main pool of heat for the Nordic Seas, where intense exchange processes between the ocean and the atmosphere are taking place [1]. Being a transit zone for warm and saline Atlantic waters on their way to the Arctic Ocean, the LB plays an important role in maintaining the Atlantic meridional overturning circulation, where the Atlantic waters transfer heat to the atmosphere, mix with the surrounding waters and undergo the transformation required for the formation of deep waters [2].

The main element of the circulation in the Norwegian Sea is the warm Norwegian Current – part of the North Atlantic Current, which is considered a system of currents consisting of two branches carrying Atlantic waters flowing through the straits between Iceland, the Faroe and the Shetland Islands. The average velocity of the Norwegian current is about 30 cm/s.

The LB feature is the quasi-permanent anticyclonic Lofoten vortex, which is located in the center of the basin and presents a natural laboratory for mesoscale eddies' study in the ocean. Deep winter convection is a necessary condition for the existence of this unique natural phenomenon, as it creates a favorable setting for annual regeneration of the Lofoten vortex [3–5]. Another mechanism that supports high anticyclonic vorticity in the center of the basin is the merging with mesoscale anticyclonic eddies that break away from the Norwegian current [6, 7]. In fig. 1 the dashed line indicates the region of the most likely location of the Lofoten vortex [7] limited to 69–71° N, 1–5° E, hereinafter the LV zone.

Apparently, it would not be a great exaggeration to say that the most important component of the LB dynamics is mesoscale eddy activity. Being formed as a result of the dynamic instability of the Norwegian current [8], they redistribute the warm and saline water of the Norwegian current over the basin's water area. Thus, the eddies play an important role in the formation of the thermohaline patterns of the LB.

On satellite altimetry maps, the LB is distinguished by raised dispersion of sea level fluctuations [9]. The maximum average value of the standard deviation is 15 cm in the center of the basin and refers to the Lofoten vortex [10]. However, as we will see later, in the LB, mesoscale eddies are formed almost everywhere. Figure 2 shows that the sea level surface represents an area, where mesoscale patterns correspond to mesoscale eddies that have different polarity and non-zero relative vorticity. In the LB, mesoscale eddies generate, dissipate, move, and interact with each other. Despite the fact that mesoscale eddies form almost everywhere in the World Ocean [11], the eddy activity regions are, in some way or other, associated with the areas of large-scale currents, such as the Norwegian current, due to the presence of baroclinic and barotropic instability, which is one of the necessary conditions for the generation of eddies [12].

The development of satellite oceanology, altimetry products in particular, as well as the growth of available computing power, lead to the rapid development of automatic algorithms of eddies' detection and tracking, which allows obtaining new information about the dynamic and kinematic characteristics of eddies. A detailed review of these algorithms is given in [13]. Among the many different methods of automatic identification, the most popular is the algorithm for detection and tracking of eddies, applied to the sea level anomalies (see, for example, [11]).

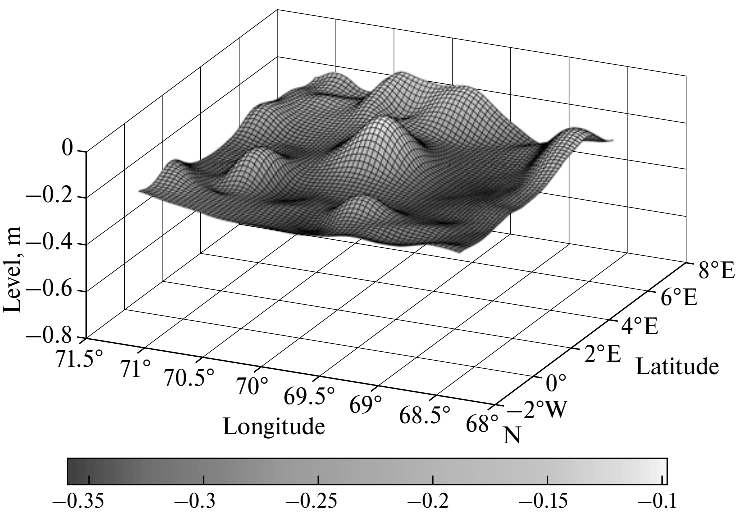

Рис. 2. Динамическая поверхность уровня океана (м) Лофотенской котловины по данным спутниковой альтиметрии за 12 декабря 2001 г.

Fig. 2. Dynamic surface sea level (m) in the LB according to altimetry data for December 12, 2001.

Our study aims to analyze the spatial distribution of mesoscale eddies in the LB, to identify the places of their generation and dissipation, as well as a statistical analysis of their characteristics. The study is based on the automatic method of identification using altimetry.

Data and methods

Altimetric measurements of sea level anomalies (SLA) are available on the CMEMS (Copernicus Marine environment monitoring service, http://marine.copernicus.eu[1]). This altimetric product is part of the European Ssalto/Duacs project, distributed by the AVISO-CNES Data Center (https://www.aviso.altimetry.fr/[2]). Altimetry measurements were obtained from Topex/Poseidon and Jason (repeat cycle of 10 days), GFO (17 days), ERS-1, ERS-2, and Envisat (35 days) satellites. The data were corrected considering the tidal influence, and various effects of the atmosphere, troposphere, and ionosphere. We used regular grid data with a spatial resolution of 0.25° latitude and longitude for the period 1993–2017.

We tested several methods of automatic eddy identification [11], [14], [15]. In this work, we used the method of automatic identification and tracking of mesoscale eddies developed by Faghmous et al. [15]. This method detects eddies as closed contours and applied to the altimetry data. Faghmous et al. [15] during the development of the algorithm, provided the identification of eddies for the World Ocean for the period from January 1993 to May 2014 and presented results in the open-access. However, we extended the study period until the end of 2017. To implement the algorithm, we used the open-source code, which was made accessible by the authors of the method on the website: https://github.com/jfaghm/OceanEddies[3].

The essence of the identification algorithm is as follows. Its basis is the assumption that only one extremum in the eddy's contour exists (minimum or maximum, depending on the type of the eddy). The extremum is defined as a grid cell, the value of which is below (for the minimum) or above (for the maximum) the other values in the specified neighborhood. The choice of a neighborhood is made on a uniform grid, to which the initial data have been previously interpolated. The contour is determined by step-by-step iterations of an increase or decrease in the critical sea level anomalies inside the contour with a step defined by the user until the assumption of a single extremum within the contour is violated, and then the eddy is indicated by the contour computed at the previous iteration. This method may lead to the size overestimation of an eddy, but with the correct choice of the iterative step, the error is not so significant. The algorithm identifies and processes the eddy formations of cyclonic and anticyclonic type separately, calculating for each of them the following parameters: the eddy's radius, amplitude (elevation or drop of the sea level at the extremum), the area inside the contour and azimuthal velocity.

After identification of all the eddies, the procedure for eddies' tracking in space and time is applied. To limit the search region, the algorithm estimates the probable velocity of the eddy's drift, defining it as the phase velocity of a long (non-dispersive) Rossby baroclinic wave within the long-wave approximation, considering the Rossby baroclinic radius [16]. A physical significance for the structures association procedure at times t and $t + 1$ is provided by the comparison of their external parameters, i.e. size and amplitude. Structures are associated when, for each of the compared parameters, the ratio of the value at the subsequent time point to the previous is in the range from 0.25 to 2.75. Sometimes, due to the noise and errors present in the initial data, the eddies may temporarily disappear, so to sustain the integrity of the track, the authors have provided the possibility of creating a "fake eddy". A "fake

[1] Access date 7 March 2019.
[2] Access date 7 March 2019.
[3] Access date 7 March 2019.

eddy" is a copy of the last observed eddy (size, amplitude, etc.) moving along the last observed real trajectory with the same velocity. It is tagged with a special mark for further exclusion during subsequent processing. In case the "fake eddy" is not succeeded by a real eddy, the track is cut off by the last eddy, identified by the procedure, as real.

We applied identification algorithm by Faghmous et al. [15] to the SLA data, available at http://marine.copernicus.eu.

Results

In total, in the studied region (fig. 1), for the period from 1993 to 2017, we allocated 166,000 cyclonic and 169,395 anticyclonic cases of the eddies' manifestation. Further, the function of binding to tracks was applied to all detected eddy formations. Thus, for the entire study period, 22,090 anticyclonic and 23,242 cyclonic eddy tracks were identified, i.e. trajectories of individual eddies. To exclude short-lived eddies related to mesoscale variability, as well as errors that may occur due to the small discreteness of satellite data in the studied area, tracks with a lifetime of fewer than 35 days (99% of the eddies) were discarded. Further analysis was carried out for tracks from the remaining long-lived 120 cyclonic and 210 anticyclonic eddy formations.

To analyze the features of the mesoscale eddies in the LB and to identify their possible linkage with the LV zone (see fig. 1), all the tracks were divided into 4 main groups depending on the generation and dissipation points of the eddies:

Group 1: eddies that appeared and disintegrated in the LV zone;

Group 2: eddies that appeared and disintegrated outside the LV zone;

Group 3: eddies moving into the LV zone from the outside;

Group 4: eddies that drift from the LV zone.

Figure 3 (see Insert) shows the cyclonic (CEs) and anticyclonic (ACEs) eddies' tracks for 4 groups, and table 1 shows their distribution within groups as a percentage. From table 1 it is apparent that for all long-lived mesoscale eddies in the LB, the second type is predominant, i.e. eddies that appeared and faded outside the LV zone. This is easily explained because the area of the LB is significantly larger than the LV zone (fig. 1). In the spatial structure of the eddies' distribution, it is clear that ACEs are formed mostly in the frontal zone of the Norwegian current, disintegrating not very far from the place of their formation, while CEs can form in different places of the water area. Note that in the western, extensive part of the water area of the Lofoten depression, there are significantly fewer eddies than in other parts of the basin (fig. 3, *a*, *b*).

The Group 1 is in the second place. We mean here eddies that appeared and disappeared in the LV zone. The majority of these eddies is represented by ACEs since those constitute the "body" of the Lofoten Vortex. Emerging, ACEs rotate intensively within the LV zone in the anticyclonic circulation, gradually merging with the Lofoten Vortex. However, cyclonic eddies are also found in the LV zone in sufficient numbers, localized mainly in the vicinity of two points with centers of 69.5° N, 4° E, and 70° N, 2.5° E. These cyclonic eddies surrounding the quasi-permanent anticyclonic Lofoten Vortex, and, as a rule, long-lived, are formed not far from the Lofoten Vortex, in the area with opposite (cyclonic) vorticity, therefore the Lofoten Vortex is so-called "shielded" vortex. "Shielded" vortices are frequently observed in nature: an anticyclonic vortex consists of a core surrounded by a powerful ring with the vorticity of the opposite sign, called "the shield" [17], [18].

The greatest interest attract eddies within Group 3 (eddies coming into the LV zone from the outside) (fig. 3, *e*, *f*). It turned out that eddies of this type are too few, only 5% (19 cases out of a total 330). Note that these eddies, generated in the region of the Norwegian current, tend to the cyclonic rotation.

Group 4 has very few eddies (table 1). Nevertheless, we believe it is important to point out that there are some eddies that move against topography.

Table 1

Distribution of mesoscale eddies by groups, %

Распределение мезомасштабных вихрей ЛК по группам, %

Groups	Types of eddies	
	CEs, 120 individual eddies	ACEs, 210 individual eddies
1	14.3%	26.2%
2	73.3%	69.5%
3	9.2%	3.8%
4	3.3%	0.5%

Thus, the analysis of the spatial structure of the mesoscale eddies in the LB made it possible to establish that there are two predominant, weakly related with each other, systems of mesoscale eddies that can reflect a different mechanism of their generation:

1) separation from the Norwegian current during its meandering;

2) generation of eddies directly in the LB.

Figure 3 demonstrates that there are three different areas of mesoscale eddy generation in the frontal zone of the Norwegian current, and they located in the vicinities of 68° N, 8° E; 69.5° N, 11° E and 71° N, 16° E, from where the eddies move to the west and north-west, forming three main trajectories (see fig. 3, *c*, *d*).

Table 2 and fig. 4 show statistical estimates of the mesoscale eddies' characteristics in the LB identified by the method [15]. It can be seen that among the long-lived (life-span more than 35 days) eddies, anticyclonic eddies dominate (almost double). On average, they have a slightly larger amplitude (6.2 cm), azimuthal speed (7.7 cm/s) and lifetime (51 days) than cyclonic eddies have, they also have the same radii (55 km) and the speed of movement along the tracks (4 km/day).

Table 2

Statistical parameters of CEs and ACEs in the LB for 1993–2017

Статистические параметры характеристик циклонических (CEs) и антициклонических (ACEs) мезомасштабных вихрей на треках в Лофотенской котловине в период 1993–2017 гг.

Characteristic	Type of eddy	Statistical parameter				
		Mean	Median	Root mean square	Minimum	Maximum
Radius, km	CEs	55.0	53.3	15.8	24.3	122.9
	ACEs	55.1	53.0	15.6	24.3	136.2
Amplitude, cm	CEs	5.2	4.2	3.5	1.0	29.3
	ACEs	6.2	5.0	4.3	1.0	26.6
Azimuthal velocity, cm/s	CEs	28.2	6.2	46.6	0.5	348.6
	ACEs	32.3	7.7	54.0	0.6	395.1
Lifetime, days	CEs	46.4	43.0	10.2	35.0	80.0
	ACEs	50.8	46.0	16.6	35.0	131.0
Moving speed, km/day	CEs	4.0	3.1	3.2	0.0	21.4
	ACEs	4.0	3.1	3.1	0.0	21.2

Figure 4 presents statistical estimates for each of the four groups, separately for cyclonic (CEs) and anticyclonic (ACEs) eddies: mean values and range of variability (box-and-whiskers) of amplitude, radius, azimuthal velocity, speed of movement, and a lifetime. Some statistical parameters of the four groups of eddies differ slightly (radius, speed of movement), and some differ significantly (for example, azimuthal speed). It is worth noting that amplitudes, the radius and azimuthal speed of the anticyclonic eddies from the Group 1 are slightly bigger, compared with the similar characteristics of eddies from other Groups and cyclonic eddies of the same group. At the same time, the moving speed differ very slightly, both between groups and the types of eddies.

Raj et al. [19] conducted a comprehensive analysis of the mesoscale eddies of the LB based on altimetry data, profiling Argo buoys and surface drifters for 1995–2013, highlighting main areas of the eddy generation: the LV zone and the periphery of the Norwegian current. The average velocity of eddies according to altimetry data for 1995–2013 using a hybrid identification algorithm, Raj et al. [19] estimated 5–6 km/day. Our results obtained from altimetry data for the period 1993–2017 refine these estimates, but also characterize in more detail the spatial distribution of the eddies during their life cycle. A comparison with the results of [19], [20] led to the conclusion that the identification algorithm [15] works well.

Raj et al. [19], [20] also revealed that anticyclonic eddies live longer than cyclonic eddies in the LB. The longest-lived anticyclonic eddies live mainly in the LV zone, which, according to assumption [19], [20], is due to the stabilizing effect of bottom topography. The relationship of stability with topography was established in [21]. In a study [19], cyclonic eddy drift was detected in the LB. In our study, this fact relates primarily to the eddies of Group 3. Thus, our analysis based on satellite data using the automatic method of identification and tracking of eddies allowed expansion of the conclusions obtained in earlier studies. The spatial distribution of mesoscale eddies in the LB was studied, the locations of their generation and dissipation were identified, and statistical analysis of the characteristics of long-lived eddies for 4 regions of the basin was carried out.

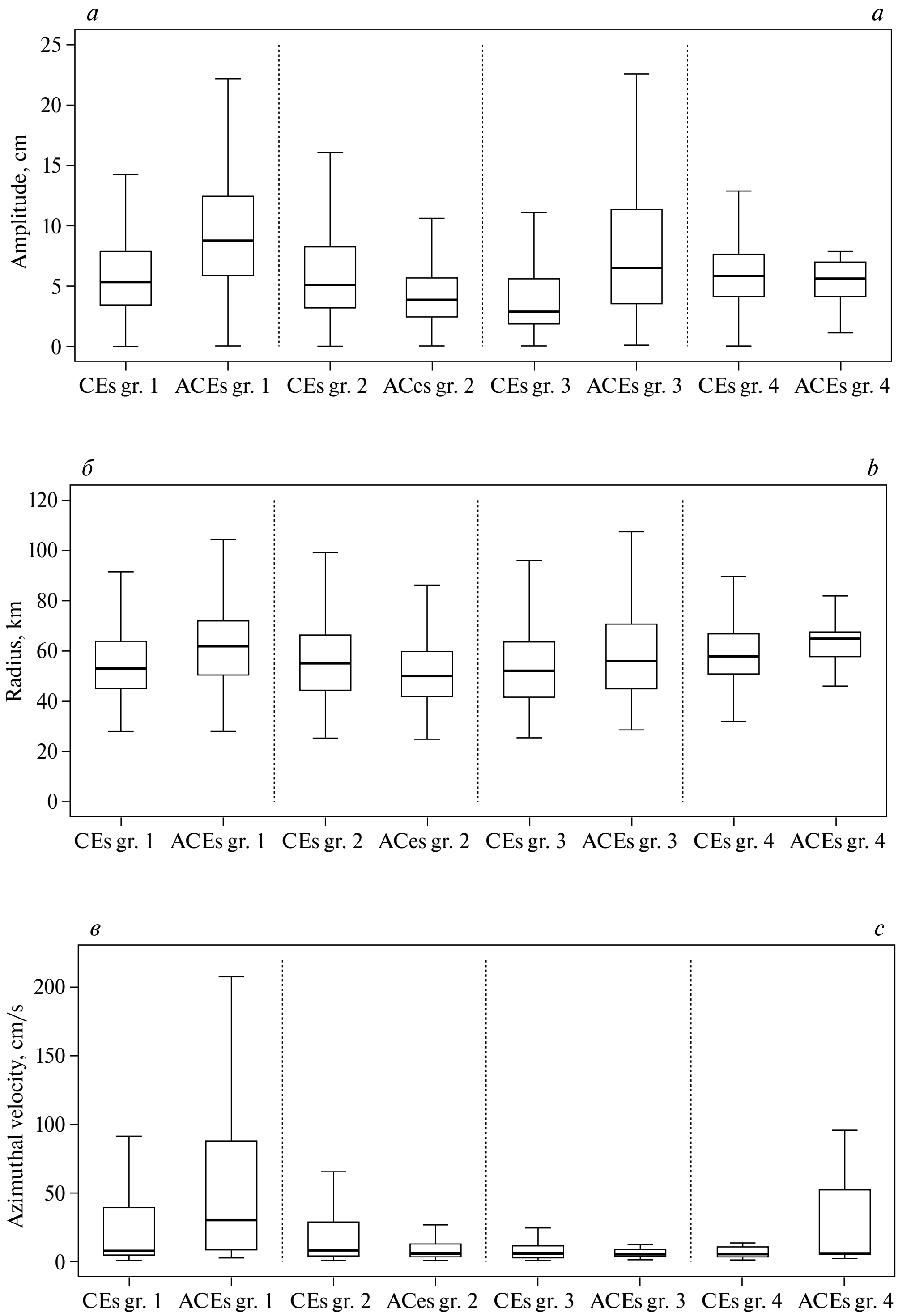

Рис. 4. «Ящики с усами» значений характеристик мезомасштабных вихрей Лофотенской котловины. *Слева* – циклонические вихри (CEs), *справа* – антициклонические (ACEs); *а* – амплитуда, см; *б* – радиус, км; *в* – азимутальная скорость, см/с; *г* – скорость перемещения по треку, км/сут.; *д* – время жизни.

Fig. 4. “Box-and-whiskers” diagrams for parameters of mesoscale eddies in the LB. Cyclonic eddies (CEs) are on the left, and anticyclonic eddies (ACEs) are on the right; *a* – the amplitude, cm; *b* – the radius, km; *c* – the azimuthal velocity, cm/s; *d* – speed of movement, km/day; *e* – life time.

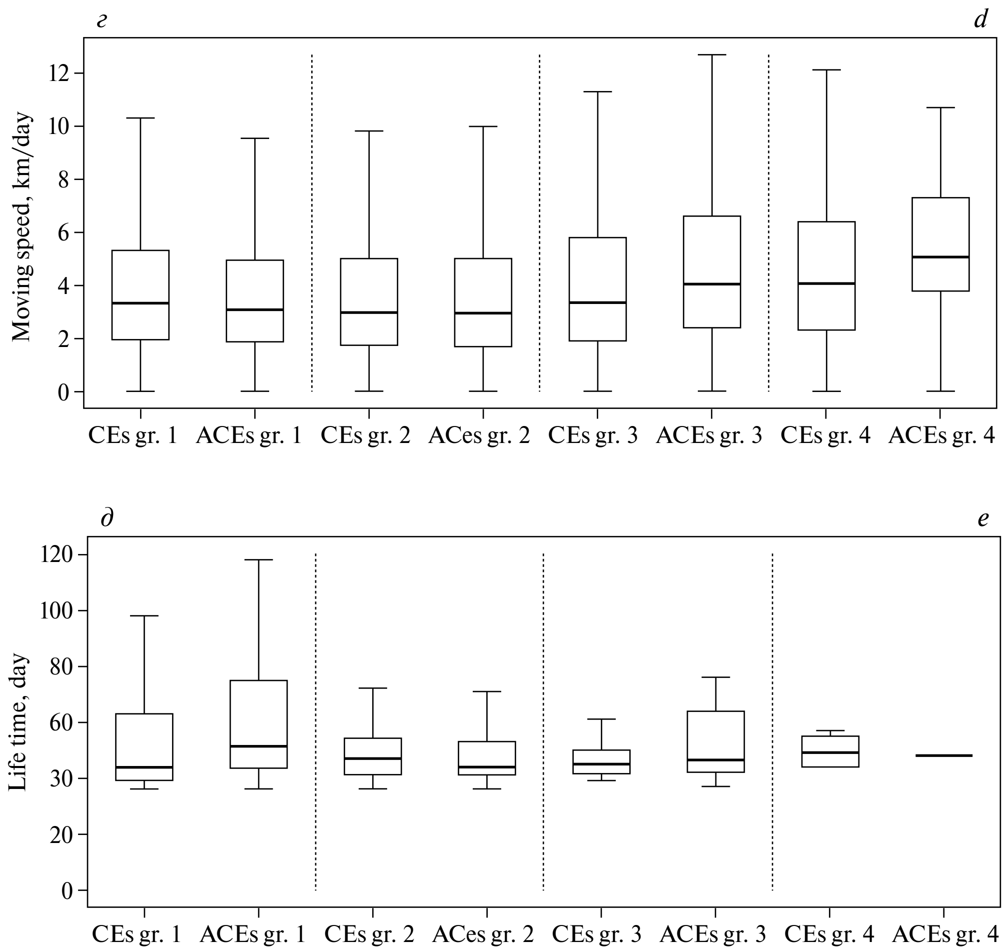

Рис. 4. (Окончание).

Fig. 4. (Ending).

Conclusion

Among the long-lived (more than 35 days) eddy formations in the Lofoten Basin, anticyclonic eddies are predominant (almost doubled). On average, anticyclonic eddies have slightly larger values of characteristics than cyclonic eddies: amplitude (6.2 cm), azimuth velocity (7.7 cm/s) and lifetime (51 days). They have the same radii with cyclonic eddies (55 km) and drift velocities along the track (4 km/day).

In the LB, there are two predominant, weakly interconnected, systems for the mesoscale eddies' formation, which may reflect various mechanisms of eddy generation: breaking from the Norwegian current during its meandering and the generation of eddies in the LB directly.

In the frontal zone of the Norwegian current, there are three distinct areas of eddies' generation, from where they move to the west and north-west, forming three main trajectories.

Anticyclonic eddies' formations dominate in the LV zone. Emerging, they rotate intensively within the LV zone in the anticyclonic gyre/circulation and, apparently, interact with the Lofoten Vortex by merging. However, cyclonic eddies in the LV zone are also found in sufficient numbers and localized in the vicinity of two points with centers of 69.5° N, 4° E and 70° N, 2.5° E. These cyclonic eddies, as a rule, are long-lived and are located in an area with opposite vorticity, surrounding the Lofoten Vortex (shielded vortex).

Mesoscale eddies that enter the LV zone from the outside are formed mainly in the area of the Norwegian current and tend to the cyclonic rotation.

Our study allowed systematization of eddies in the LB into groups reflecting different generation mechanisms.

Using the algorithm of automatic identification and tracking of mesoscale eddies, we have demonstrated that anticyclonic eddies in the LB are formed mostly in the frontal zone of the Norwegian current, decaying not very far from the place of its generation while cyclonic eddies may form in different places in the LB.

In the western part of the LB, the number of eddies is much smaller than in other its areas. We studied this aspect obtaining quantitative estimates of the number of eddies, analyzing their characteristics and examining the areas of their generation and dissipation using satellite altimetry data.

Acknowledgments

This work was supported by the Russian Science Foundation, grant No. 18-17-00027. The authors express their sincere gratitude to two anonymous reviewers for in-depth analysis of the article and valuable comments that contributed to the improvement of its quality.

Литература

1. *Rossby T.*, *Ozhigin V.*, *Ivshin V.*, *Bacon S.* An isopyncal view of the Nordic seas hydrography with focus on properties of the Lofoten Basin // Deep-Sea Res. I. 2009. 56. P. 1955–1971.
2. *Richards C.G.*, *Straneo F.* Observations of Water Mass Transformation and Eddies in the Lofoten Basin of the Nordic Seas // J. Phys. Oceanogr. 2015. 45. P. 1735–1756. https://doi.org/10.1175/JPO-D-14-0238.1
3. *Блошкина Е.В.*, *Иванов В.В.* Конвективные структуры в Норвежском и Гренландском морях по результатам моделирования с высоким пространственным разрешением // Труды Гидрометеорологического научно-исследовательского центра Российской Федерации. 2016. 361. С. 146–168.
4. *Bashmachnikov I.L.*, *Sokolovskiy M.A.*, *Belonenko T.V.*, *Volkov D.L.*, *Isachsen P.E.*, *Carton X.* On the vertical structure and stability of the Lofoten vortex in the Norwegian Sea // Deep-Sea Res. I, 2017. 128. P. 1–27. http://dx.doi.org/10.1016/j.dsr.2017.08.001
5. *Федоров А.М.*, *Башмачников И.Л.*, *Белоненко Т.В.* Зимняя конвекция в Лофотенской котловине по данным буев ARGO и гидродинамического моделирования // Вестник СПбГУ. Науки о Земле. 2019. 64 (3), 491—511. https://doi.org/10.21638/spbu07.2019.308
6. *Köhl A.* Generation and Stability of a Quasi-Permanent Vortex in the Lofoten Basin // J. Phys. *Oceanogr.* 2007. 37. 2637–2651.
7. *Volkov D.L.*, *Kubryakov A.A.*, *Lumpkin R.* Formation and variability of the Lofoten basin vortex in a high-resolution ocean model // Deep-Sea Res. I. 2015. 105. P. 142–157. https://doi.org/10.1016/j.dsr.2015.09.001
8. *Isachsen P.E.* Baroclinic instability and the mesoscale eddy field around the Lofoten Basin // J. Geophys. Res. 2015. 120(4). P. 2884–2903.
9. *Белоненко Т.В.*, *Волков Д.Л.*, *Норден Ю.Е.*, *Ожигин В.К.* Циркуляция вод в Лофотенской котловине Норвежского моря // Вестник СПбГУ. 2014. 7 (2). С. 108–121.
10. *Volkov D.L.*, *Belonenko T.V.*, *Foux V.R.* Puzzling over the dynamics of the Lofoten Basin – a sub-Arctic hot spot of ocean variability // Geophys. Res. Lett. 2013. 40, 4. P. 738–743. doi:10.1002/grl.50126
11. *Chelton D.B.*, *Gaube P.*, *Schlax M.G.*, *Early J.J.*, *Samelson R.M.* The influence of nonlinear mesoscale eddies on near-surface oceanic chlorophyll // Science. 2011. V. 334, N 6054. P. 328–332.
12. *Монин А.С.*, *Жихарев Г.М.* Океанские вихри // Успехи физических наук. 1990. Т. 160, Вып. 5. С. 1–47.
13. *Петкилёв П.С.* Обзор алгоритмов обнаружения и трекинга мезомасштабных вихрей // Современные проблемы дистанционного зондирования Земли из космоса. 2017. Т. 14, № 3. С. 129–149.
14. *Nencioli F.*, *Dong C.*, *Dickey T.*, *Washburn L.*, *McWilliams J.C.* A Vector Geometry-Based Eddy Detection Algorithm and Its Application to a High-Resolution Numerical Model Product and High-Frequency Radar Surface Velocities in the Southern California Bight // Journal of Atmospheric and Oceanic Technology. 2010. 27. P. 564–579.
15. *Faghmous J.H.*, *Frenger I.*, *Yao Y.*, *Warmka R.*, *Lindell A.*, *Kumar V.* A daily global mesoscale ocean eddy dataset from satellite altimetry // Sci. Data. 2015. N 2. P. 150028. DOI:10.1038/sdata.2015.28
16. *Chelton D.B.*, *DeSzoeke R.A.*, *Schlax M.G.* Geographical variability of the first baroclinic Rossby radius of deformation // Journal of Physical Oceanography. 1998. V. 28, N 3. P. 433–460.
17. *Carton X.J.* On the Merger of Shielded Vortices // EPL (Europhysics Letters). 1992. 18(8). DOI: https://doi.org/10.1209/0295-5075/18/8/006
18. *Tóth G.*, *Házi G.* Merging of shielded Gaussian vortices and formation of a tripole at low Reynolds numbers // PHYSICS OF FLUIDS. 2010. 22, 053101. DOI:10.1063/1.3428539
19. *Raj R.P.*, *Johannessen J.A.*, *Eldevik T.*, *Nilsen J.E.Ø.*, *Halo I.* Quantifying mesoscale eddies in the Lofoten Basin // J. Geophys. Res. Oceans. 2016. N 121. P. 4503–4521. DOI:10.1002/2016JC011637
20. *Raj R.P.*, *Chafik L.*, *Nilsen J.E.Ø*, *Eldevik T.*, *Halo I.* The Lofoten Vortex of the Nordic Seas, in: Deep-Sea Res. // 2015. 196. P. 1–14.
21. *Bashmachnikov I.L.*, *Sokolovskiy M.A.*, *Belonenko T.V.*, *Volkov D.L.*, *Isachsen P.E.*, *Carton X.* On the vertical structure and stability of the Lofoten vortex in the Norwegian Sea // Deep-Sea Res. I. 2017. 128. P. 1–27. http://dx.doi.org/10.1016/j.dsr.2017.08.001

References

1. *Rossby T., Ozhigin V., Ivshin V., Bacon S.* An isopyncal view of the Nordic seas hydrography with focus on properties of the Lofoten Basin. *Deep-Sea Res.* I, 2009, 56, 1955–1971.
2. *Richards C.G., Straneo F.* Observations of Water Mass Transformation and Eddies in the Lofoten Basin of the Nordic Seas. *J. Phys. Oceanogr.* 2015, 45, 1735–1756. https://doi.org/10.1175/JPO-D-14–0238.1
3. *Bloshkina E.V., Ivanov V.V.* Convective structures in the Norwegian and Greenland Seas based on simulation results with high spatial resolution. *Proceedings of the Hydrometeorological Research Center of the Russian Federation*. 2016, 361, 146–168 (in Russian).
4. *Bashmachnikov I.L., Sokolovskiy M.A., Belonenko T.V., Volkov D.L., Isachsen P.E., Carton X.* On the vertical structure and stability of the Lofoten vortex in the Norwegian Sea. *Deep-Sea Res.* I, 2017, 128, 1–27. http://dx.doi.org/10.1016/j.dsr.2017.08.001
5. *Fedorov A.M., Bashmachnikov I.L., Belonenko T.V.* Winter convection in the Lofoten Basin according to ARGO buoys and hydrodynamic modeling. *Vestnik S.-Petersbur. Un-ta, Earth Sciences*. 2019, 64 (3), 491–511. https://doi.org/10.21638/spbu07.2019.308 (in Russian).
6. *Köhl A.* Generation and Stability of a Quasi-Permanent Vortex in the Lofoten Basin. *J. Phys. Oceanogr.* 2007, 37, 2637–2651.
7. *Volkov D.L., Kubryakov A.A., Lumpkin R.* Formation and variability of the Lofoten basin vortex in a high-resolution ocean model. *Deep-Sea Res.* I, 2015, 105, 142–157. https://doi.org/10.1016/j.dsr.2015.09.001
8. *Isachsen P.E.* Baroclinic instability and the mesoscale eddy field around the Lofoten Basin. *J. Geophys. Res.* 2015, 120(4), 2884–2903.
9. *Belonenko T.V., Volkov D.L., Ozhigin V.K., Norden Yu.E.* Circulation of waters in the Lofoten Basin of the Norwegian Sea. *Vestnik S.-Petersbur. Un-ta, Earth Sciences*. 2014, 7(2), 108–121 (in Russian).
10. *Volkov D.L., Belonenko T.V., Foux V.R.* Puzzling over the dynamics of the Lofoten Basin – a sub-Arctic hot spot of ocean variability. *Geophys. Res. Lett.* 2013, 40, 4, 738–743. DOI:10.1002/grl.50126
11. *Chelton D.B., Gaube P., Schlax M.G., Early J.J., Samelson R.M.* The influence of nonlinear mesoscale eddies on near-surface oceanic chlorophyll. *Science*. 2011, 334, 6054, 328–332.
12. *Monin A.S., Zhikharev G.M.* Ocean Vortices. *Usp. Phys.* 1990, 160 (5), 1–47.
13. *Petkilev P.S.* Review of mesoscale eddy detection and tracking algorithms. *Sovremennye Problemy Distancionnogo Zondirovanija Zemli iz Kosmosa*. 2017, 14 (3), 129–149.
14. *Nencioli F., Dong C., Dickey T., Washburn L., McWilliams J.C.* A Vector Geometry-Based Eddy Detection Algorithm and Its Application to a High-Resolution Numerical Model Product and High-Frequency Radar Surface Velocities in the Southern California Bight. *Journal of Atmospheric and Oceanic Technology*. 2010, 27, 564–579.
15. *Faghmous J.H., Frenger I., Yao Y., Warmka R., Lindell A., Kumar V.* A daily global mesoscale ocean eddy dataset from satellite altimetry. *Sci. Data*. 2015, 2, 150028. DOI:10.1038/sdata.2015.28
16. *Chelton D.B., DeSzoeke R.A., Schlax M.G.* Geographical variability of the first baroclinic Rossby radius of deformation. *Journal of Physical Oceanography*. 1998, 28, 3, 433–460.
17. *Carton X.J.* On the Merger of Shielded Vortices. *EPL* (*Europhysics Letters*). 1992, 18(8), DOI: https://doi.org/10.1209/0295-5075/18/8/006
18. *Tóth G., Házi G.* Merging of shielded Gaussian vortices and formation of a tripole at low Reynolds numbers. *PHYSICS OF FLUIDS*. 2010, 22, 053101. DOI:10.1063/1.3428539
19. *Raj R.P., Johannessen J.A., Eldevik T., Nilsen J.E.Ø., Halo I.* Quantifying mesoscale eddies in the Lofoten Basin. *J. Geophys. Res. Oceans*. 2016, 121, 4503–4521. DOI:10.1002/2016JC011637
20. *Raj R.P., Chafik L., Nilsen J.E.Ø., Eldevik T., Halo I.* The Lofoten Vortex of the Nordic Seas. *Deep-Sea Res.* 2015, 196, 1–14.
21. *Bashmachnikov I.L., Sokolovskiy M.A., Belonenko T.V., Volkov D.L., Isachsen P.E., Carton X.* On the vertical structure and stability of the Lofoten vortex in the Norwegian Sea. *Deep-Sea Res.* I, 2017, 128, 1–27. http://dx.doi.org/10.1016/j.dsr.2017.08.001

К статье *Зинченко В. А., Гордеева С. М., Собко Ю. В., Белоненко Т. В.* Мезомасштабные вихри Лофотенской котловины по спутниковым данным

Zinchenko V. A., Gordeeva S. M., Sobko Yu.V., Belonenko T. V. Analysis of Mesoscale eddies in the Lofoten Basin based on satellite altimetry

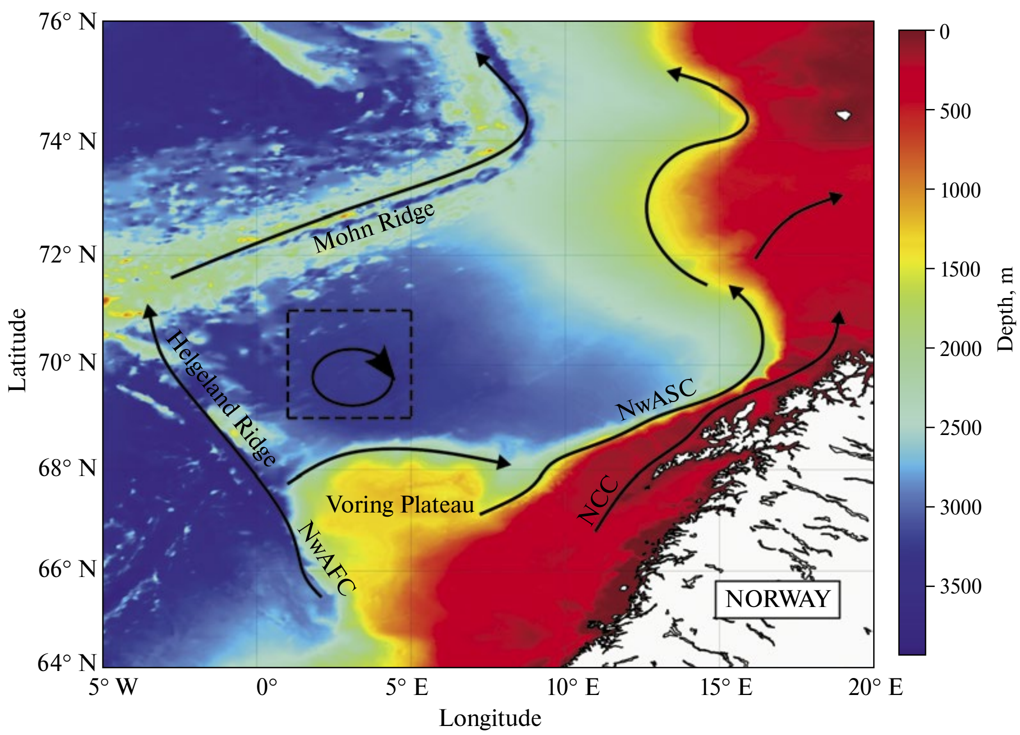

Рис. 1. Район исследования. Наиболее вероятное положение антициклонического Лофотенского вихря показано пунктиром, а он сам – круговой стрелкой. Цветом показана топография дна (м), черными стрелками – ветви Норвежского течения (используются международные обозначения [7]): Норвежское фронтальное течение (NwAFC), Норвежское прибрежное течение (NCC), Норвежское склоновое течение (NwASC).

Fig. 1. Bottom topography (colour) and general circulation (black arrows) of the study region. The dashed line marks the most likely position of the Lofoten Vortex; the location of the Lofoten Vortex shown with the circle. Abbreviations [7]: NCC is the Norwegian Coastal Current, NwASC is the Norwegian Atlantic Slope Current, NwAFC is the Norwegian Atlantic Frontal Current.

К статье *Зинченко В. А., Гордеева С. М., Собко Ю. В., Белоненко Т. В.* Мезомасштабные вихри Лофотенской котловины по спутниковым данным

Zinchenko V. A., Gordeeva S. M., Sobko Yu.V., Belonenko T. V. Analysis of Mesoscale eddies in the Lofoten Basin based on satellite altimetry

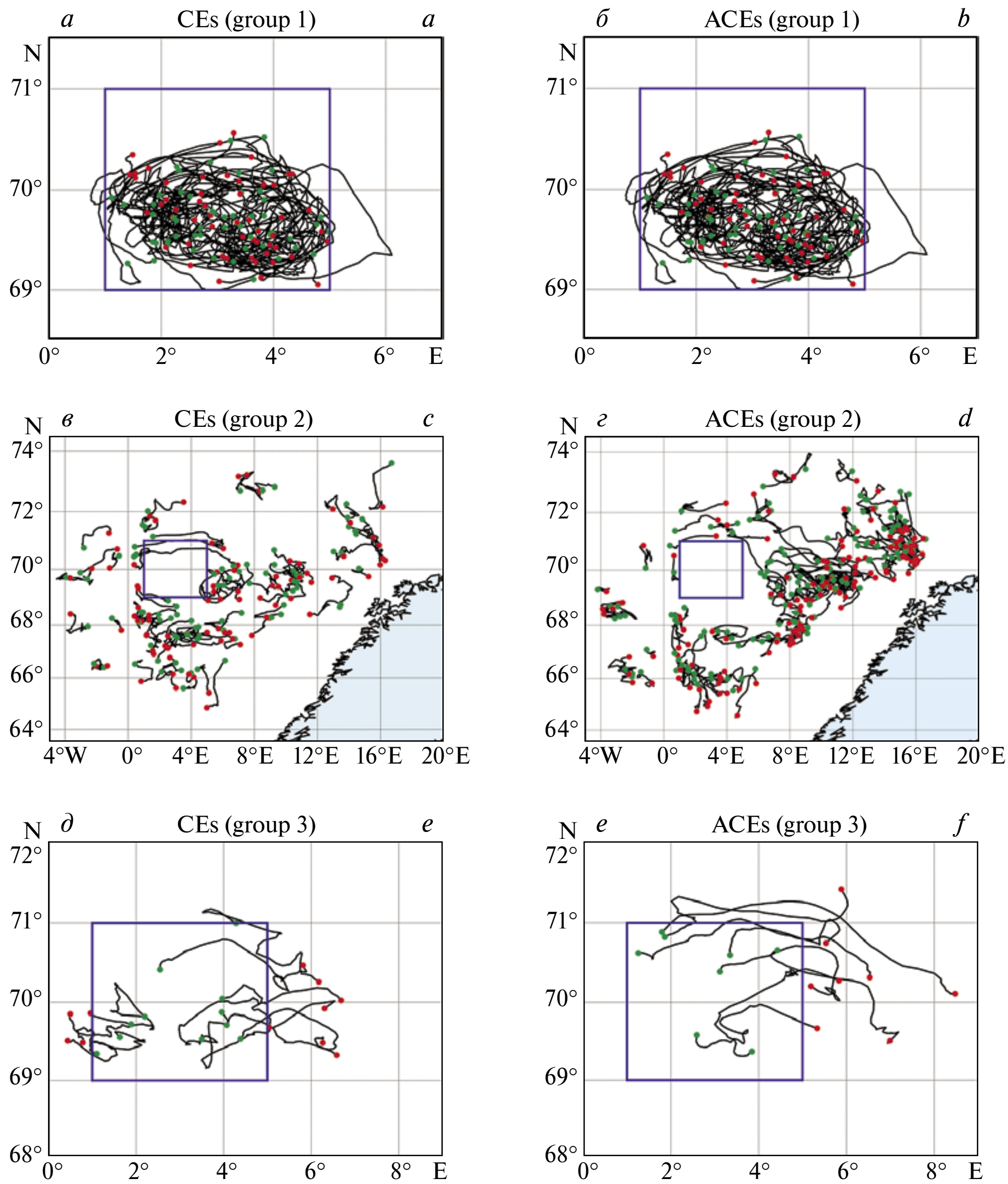

Рис. 3. Распределение треков мезомасштабных вихрей в Лофотенской котловине по 4 группам; красными точками показано местоположение генерации вихрей, зеленые указывают на место их диссипации.

Fig. 3. Spatial distribution of tracks for 4 groups of mesoscale eddies in the LB; the red dots indicate the location of the eddy generation, and the green ones denote the place of their dissipation.

К статье *Зинченко В. А., Гордеева С. М., Собко Ю. В., Белоненко Т. В.* Мезомасштабные вихри Лофотенской котловины по спутниковым данным

Zinchenko V. A., Gordeeva S. M., Sobko Yu.V., Belonenko T. V. Analysis of Mesoscale eddies in the Lofoten Basin based on satellite altimetry

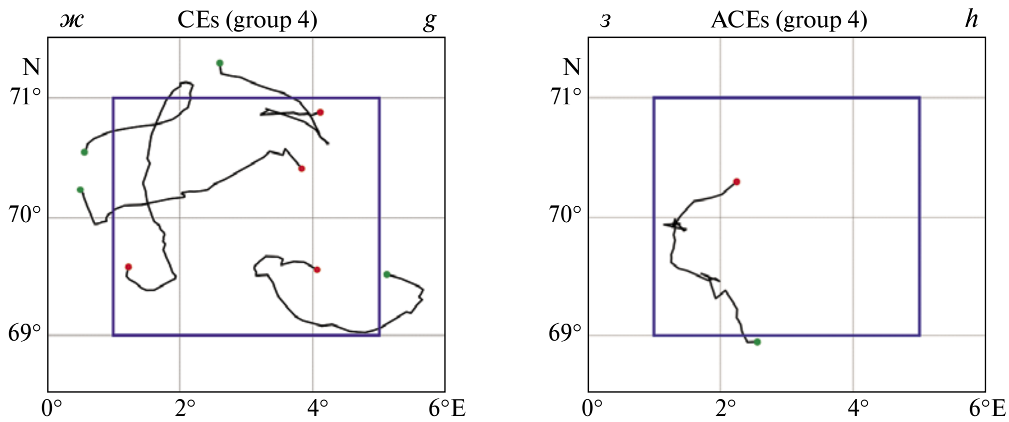

Рис. 3. (Окончание).

Fig. 3. (Ending).